

Crystal Structure, Thermal Behaviour and Vibrational Spectra of Tetraethylammonium Dihydrogenmonophosphate Bis Phosphoric Acid

Ikram Dhouib^{1*}, Salih Al-Juaid², Tahar Mhiri¹, Zakaria Elaoud¹

¹Laboratoire de l'Etat Solide, Département de Chimie, Faculté des Sciences de Sfax, Sfax, Tunisia

²Chemistry Department, Faculty of Science, King Abdulaziz University, Jeddah, KSA
Email: *ikramdhouib82@yahoo.fr

Received January 18, 2013; revised February 25, 2013; accepted March 3, 2013

ABSTRACT

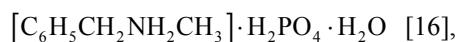
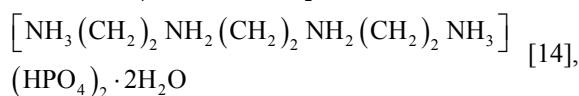
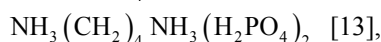
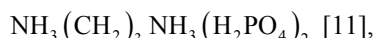
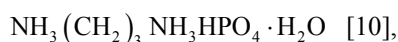
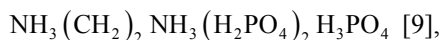
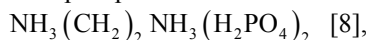
Single crystals of the tetraethylammonium dihydrogenmonophosphate bis trihydrogenmonophosphate $[\text{CH}_3\text{CH}_2]_4\text{N}^+(\text{H}_2\text{PO}_4^-)(\text{H}_3\text{PO}_4)_2$ (TEP), were grown by slow evaporation solution technique at room temperature. The compound was characterised by IR, Raman, differential thermal analysis (TG-DTA) and single crystal X-ray diffraction. It crystallizes in the monoclinic system (space group $P2_1/c$) with the following unit cell dimensions: $a = 7.765$ (2) Å, $b = 16.531$ (4) Å, $c = 14.843$ (2) Å, $\beta = 100.99$ (2)°, $Z = 4$, $D_x = 1.67\text{Mg}\cdot\text{m}^{-3}$, $D_m = 1.532\text{Mg}\cdot\text{m}^{-3}$, λ (MoK α) = 0.71073 Å, $\mu = 0.384\text{mm}^{-1}$, $F(000) = 991$, $T = 20$ (2)°. The structure was solved by the direct method and refined to final R value of 0.0342 and $R_w = 0.107$ for 3239 independent reflections. The structure consists of infinite parallel two-dimensional planes built of mutually H_2PO_4^- , H_3PO_4 tetrahedra and $[(\text{CH}_3\text{CH}_2)_4\text{N}]^+$ cations connected by strong O-H...O and C-H...O hydrogen bonding. There are no contacts other than van der Waals interactions between the layers.

Keywords: Organic Phosphate; Crystalline Structure; Vibrational Spectra; Thermal Behaviour; Differential Thermal Analysis.

1. Introduction

In organic-cation monophosphates, the phosphate anions generally observed are the acidic ones $[\text{HPO}_4]^{2-}$ or $[\text{H}_2\text{PO}_4]^-$. Such anions are interconnected by strong hydrogen bonds so as to build infinite networks with various geometries: ribbons [1], chains [2,3], two-dimensional network [4-6], and three-dimensional network [7]. These entities can be associated to organic molecules to produce compounds having a particular interest as non-linear optical materials.

During a systematic investigation of interactions between monophosphoric acid and organic molecules containing one or more nitrogen atom different structures of monophosphate salts have been described:



In the present work we describe the chemical preparation, the crystal structure, calorimetric measurements and Fourier transform infrared (FTIR) spectral characterization of a new compound: the tetraethylammonium dihydrogenmonophosphate bis trihydrogenmonophosphate $[\text{CH}_3\text{CH}_2]_4\text{N}^+(\text{H}_2\text{PO}_4^-)(\text{H}_3\text{PO}_4)_2$, here after abbreviated to (TEP), which is a close analogue of previously ob-

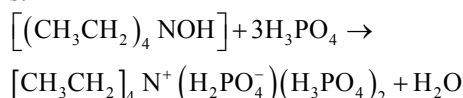
*Corresponding author.

tained $[\text{CH}_3\text{CH}_2]_4\text{N}^+(\text{H}_2\text{AsO}_4^-)(\text{H}_3\text{AsO}_4)_2$ [19].

2. Experimental

2.1. Synthesis

The crystal of TEP is easily prepared by slow evaporation at room temperature of an aqueous solution of H_3PO_4 and $[(\text{CH}_3\text{CH}_2)_4\text{NOH}]$. Schematically the reaction is:



After some days of evaporation, colorless needle-shaped monocrystals appear in the solution. The chemical analysis of phosphorus and acidic proton has been carried out [20].

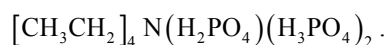
Density was measured at room temperature by flotation in toluene. The average value of density,

$$D_m = 1.532 \text{ Mg} \cdot \text{m}^{-3},$$

is agreement with that calculated,

$$D_x = 1.598 \text{ Mg} \cdot \text{m}^{-3}.$$

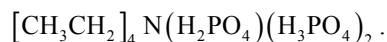
The cell contains two formula units of



2.2. Characterizations

The infrared spectrum was recorded in the range 400–4000 cm^{-1} with a “Perkin Elmer FTIR-1000” spectrophotometer using a sample dispersed in a KBr pellet. Back scattering Raman spectra were obtained under microscope with a Horiba Jobin Yvon Raman spectrometer (Lab RAM HR 800 $\lambda = 633 \text{ nm}$) in the 50–4050 cm^{-1} range.

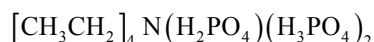
Setaram thermoanalyser, TG-DTA92, was used to perform thermal treatment on samples of



TG-DTA thermograms were obtained with 34.35 mg sample in an open platinum crucible, heated in air with $5^\circ\text{C} \cdot \text{min}^{-1}$ heating rate, from room temperature to 275°C , an empty crucible was used as reference.

2.3. X-Ray Single Crystal Structure Determination

Single-crystal X-ray data



were collected at room temperature on a Nonius Kappa-CCD diffractometer using Mo- K_α radiation $\lambda = 0.71073 \text{ \AA}$ through the program COLLECT [21]. Correction for Lorentz-polarisation effect, peak integration and background determination were carried out with the program DENZO [22]. Frame scaling and unit cell parameters refinement were performed with the program

Table 1. Crystal data and summary of intensity data collection and structure refinement.

Compound	$[\text{CH}_3\text{CH}_2]_4\text{NH}_2\text{PO}_4(\text{H}_3\text{PO}_4)_2$
Color/Shape	Colourless/Parallelepiped
Molecular weight, $\text{g} \cdot \text{mol}^{-1}$	450.23
Space group	$P2_1/c$
Temp, Deg $^\circ\text{C}$	20 (2)
Unit cell dimensions (\AA)	7.765 (2)
<i>a</i> , \AA	16.531 (4)
<i>b</i> , \AA	14.843 (2)
<i>c</i> , \AA	100.99 (2)
β , $^\circ$	1870.33 (8)
Cell volume, \AA^3	4
Formula units/unit cell	1.598
D_{calc} , $\text{g} \cdot \text{cm}^{-3}$	0.384
μ_{calc} , cm^{-1}	KAPPA CAD4. Enraf-Nonius
Diffractometer/scan	Mo- K_α ($\lambda = 0.71073$)
Radiation, graphite monochromator	$0.7 \times 0.3 \times 0.3$
Max. crystal dimensions, mm	3239
Reflections measured	$-9/3, -18/19, -17/17$
Range of <i>h, k, l</i>	2506
Reflections with $F_0 > 4\sigma(F_0)^b$	$1/\sigma^2(F_0^2) + (0.0655P)^2 + 0.00P$
Weights	avec $P = (F_0^2 + 2F_c^2)/3$
GOF	1.157
$R = \sum \ F_0\ - \ F_c\ / \sum \ F_0\ $	0.0342
Rw	0.1072
T_{min}	0.7749
T_{max}	0.8935
Computer programs ^c	SHELXS-97(Sheldrick, 1990)
	SHELXL-97(Sheldrick, 1997)

SCALE-PACK [22].

Pertinent details of the crystal structure of $[\text{CH}_3\text{CH}_2]_4\text{N}(\text{H}_2\text{PO}_4)(\text{H}_3\text{PO}_4)_2$ are listed in **Table 1**. The crystal structure has been solved and refined in the monoclinic symmetry, space group $P2_1/c$, using the WINGX environment [23] and based on SHELXS97 [24] and SHELXL97 [25] softwares. All the hydrogen positions of the diprotonated cation were placed geometrically and held in the riding mode, the C-H bonds were fixed and affined at 0.78 and 1.01 \AA , respectively). Interatomic distances, bond angles and the hydrogen bonds scheme are listed in **Tables 2** and **3** respectively.

3. Results and Discussion

3.1. Structural Analysis

The asymmetric unit is composed of one $[\text{H}_2\text{PO}_4]^-$ anion, two neutral phosphoric acid $[\text{H}_3\text{PO}_4]$ and one $[(\text{CH}_3\text{CH}_2)_4\text{N}]^+$ cation. The structural arrangement of $[\text{CH}_3\text{CH}_2]_4\text{N}(\text{H}_2\text{PO}_4)(\text{H}_3\text{PO}_4)_2$ can be described as an alternation of organic $[\text{N}(\text{C}_2\text{H}_5)_4]^+$ groups and inorganic $(\text{H}_2\text{PO}_4)(\text{H}_3\text{PO}_4)_2$ is illustrated in **Figure 1**, viewed in projection along the direction of its two-fold screw axes.

One can distinguish the chains of the acid molecules and the chains of the dihydrogenphosphates anions running parallel to the Z axis in each layer (see **Figure 2**).

The molecules/anions in the chains are related to each

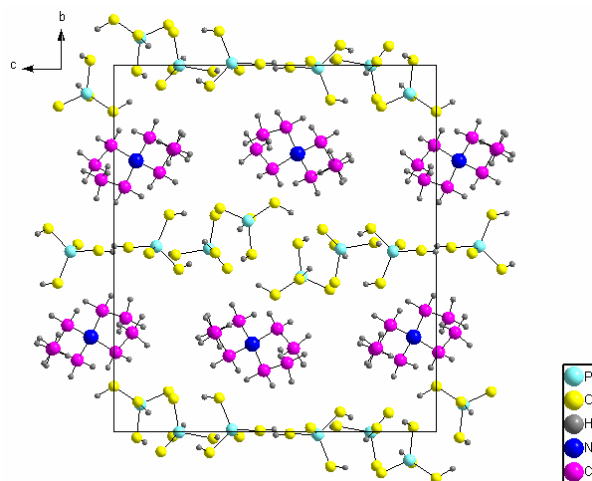
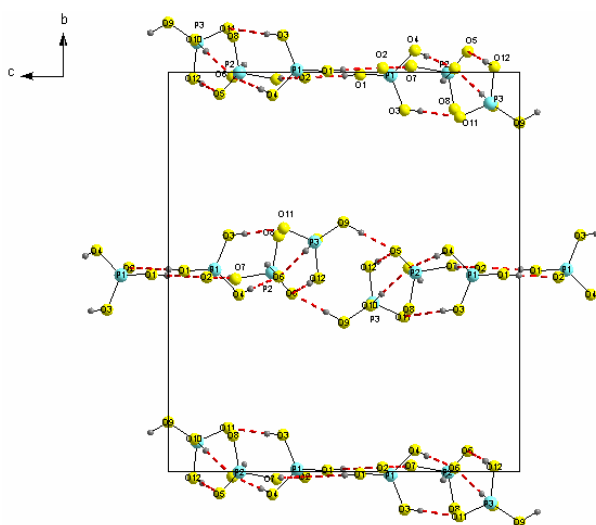
Table 2. Principal intratomic distances (Å) and bond angles (°) in $[\text{CH}_3\text{CH}_2]_4\text{N}^+(\text{H}_2\text{PO}_4^-)(\text{H}_3\text{PO}_4)_2$.

Tetrahedron around P		$[\text{CH}_3\text{CH}_2]_4\text{N}^+$ cations	
P1-O1	1.552 (2)	N-C1	1.512 (3)
P1-O2	1.496 (2)	N-C2	1.522 (3)
P1-O3	1.554 (2)	N-C3	1.526 (3)
P1-O4	1.544 (2)		
O1-H1	0.78 (5)	N-C4	1.522 (3)
O4-H4	0.84 (4)		
O3-H3	0.78 (4)		
O2-P1-O4	110.0 (1)	C1-C6	1.517 (4)
O2-P1-O1	111.54 (1)	C2-C8	1.509 (4)
O4-P1-O1	108.1 (1)	C3-C5	1.516 (3)
O4-P1-O3	108.1 (1)	C4-C7	1.517 (3)
O1-P1-O3	104.5 (1)	C1-N-C4	110.4 (2)
O2-P1-O3	113.5 (1)	C1-N-C2	107.0 (2)
P2-O5	1.511 (2)	C4-N-C2	110.9 (2)
P2-O6	1.505 (2)	C1-N-C3	111.1 (2)
P2-O7	1.56 (12)	C4-N-C3	106.5 (2)
P2-O8	1.571 (2)		
O6-H6	0.82 (1)	C2-N-C3	111.0 (2)
O7-H7	0.82 (4)		
O6-P2-O5	114.63 (9)	C8-C2-N	114.9 (2)
O6-P2-O7	106.19 (9)	C7-C4-N	114.8 (2)
O5-P2-O7	110.64 (1)	C5-C3-N	114.4 (2)
O6-P2-O8	107.63 (9)	C1-C6-N	115.1 (2)
O5-P2-O8	109.45(1)		
O7-P2-O8	108.05 (1)		
P3-O9	1.547 (12)		
P3-O10	1.540 (2)		
P3-O11	1.505 (2)		
P3-O12	1.554 (2)		
O9-H9	0.86 (4)		
O10-H10	0.78 (4)		
O12-H12	0.83 (4)		
O11-P3-O10	113.71 (9)		
O11-P3-O9	108.93 (9)		
O10-P3-O9	105.66 (9)		
O11-P3-O12	111.7 (1)		
O10-P3-O12	106.7 (1)		
O9-P3-O12	109.97 (9)		

Table 3. Principal interatomic distances (Å) and bond angles (°) and detailed of the hydrogen bonding scheme.

D-H...A	d (D-H) (Å)	d (H...A) (Å)	d (D...A) (Å)	D-H...A (angle °)
O1-H1...O2 ^v	0.78 (5)	1.81 (5)	2.578 (2)	170 (5)
O3-H3...O11	0.78 (4)	1.83 (4)	2.598 (2)	174 (5)
O4-H4...O6	0.84 (4)	1.72 (4)	2.554 (2)	171 (4)
O9-H9...O5 ⁱ	0.86 (4)	1.68 (4)	2.521 (2)	165 (4)
O7-H7...O2 ⁱⁱ	0.82 (4)	1.83 (4)	2.617 (2)	162 (4)
O10-H10...O6	0.78 (4)	1.76 (4)	2.539 (2)	177 (4)
O12-H12...O5 ⁱⁱⁱ	0.83 (4)	1.75 (4)	2.584 (2)	178 (4)
C1-H1B...O8 ^{iv}	1.01 (3)	2.37 (3)	3.315 (3)	154 (2)

Symmetry codes: ⁱ-x + 1, -y + 1, -z + 1; ⁱⁱ-x + 1, -y + 2, -z + 1; ⁱⁱⁱ-x + 2, -y + 1, -z + 1; ^{iv}x, y - 1, z; ^v-x + 2, -y + 2, -z + 1; ^{vi}x + 1, y, z.

**Figure 1. Projection along the a axis of the atomic arrangement of $[\text{CH}_3\text{CH}_2]_4\text{N}^+(\text{H}_2\text{PO}_4^-)(\text{H}_3\text{PO}_4)_2$.****Figure 2. Projection along the axis of the inorganic arrangement.**

other by the two-fold screw axis. The distance (P (1) – P (3) = 4.313 (1) Å) between two H_3PO_4 groups linked by

hydrogen bond is shortened when compared to the remaining P-P bond lengths P (1) – P (2): 4.499 (1) Å and P (2) – P(3): 4.369 (1) Å between H_3PO_4 and H_2PO_4^- groups. The $\text{H}_2\text{P}(2)\text{O}_4^-$ anions, $\text{H}_3\text{P}(1)\text{O}_4$ and $\text{H}_3\text{P}(3)\text{O}_4$ molecules are joined into trimmers by the hydrogen bonds (see **Table 3**). The dihydrogenphosphate anions $\text{H}_2\text{P}(2)\text{O}_4^-$ and the acid $\text{H}_3\text{P}(3)\text{O}_4$ molecules do not form any straight contact between themselves. All their of $\text{H}_2\text{P}(2)\text{O}_4^-$ one O-H groups are involved in the hydrogen bonds with the O(7) atoms of the acid $\text{H}_3\text{P}(1)\text{O}_4$ molecules and all their of $\text{H}_3\text{P}(3)\text{O}_4$ three O-H group are involved in the hydrogen bonds with the O(9), O(10) and O(12) of the dihydrogenphosphate anions $\text{H}_2\text{P}(2)\text{O}_4^-$.

The acid $\text{H}_3\text{P}(1)\text{O}_4$ molecules form strong ($\text{O1-H1}\cdots\text{O2}^v$) hydrogen bonds between themselves.

Note that the O(5) atoms of the dihydrogenphosphates anions participate in two hydrogen bonds with the OH groups (O(9)-H(9) and (O(12)-H(12))) of the neighbour orthophosphoric acid molecules of the same chain.

The structure is based on sheets of H_2PO_4^- and H_3PO_4 tetrahedra fused together by strong intralayer O-H \cdots O hydrogen bonds, giving to trimmers, d(O) – O < 2.73 Å [26,27]. The midplanes of these clusters, are located at $z = 0.25$ and $z = 0.75$.

The organic group of tetraethylammonium monocation structure is similar to that in the TESe and TEAs analogue [19,28]. Each tetrapropylammonium cation makes three short contacts with trimmers of the dihydrogenarsenate through the C-H \cdots O hydrogen bonds: C1-H1B \cdots O8^{iv} (see **Table 3**). The H \cdots O distance is equal to 2.37 (3) Å, respectively. The C \cdots O distance is equal to 3.315 (3) Å, showing that those hydrogen bonds are very weak [29]. The C-H \cdots O angle is equal to 154(2). The structure of the tetrapropylammonium cation is similar to that in the crystals of tetraethylammonium chloride, is in the tetraethylammonium chloride monohydrate [30], tetraethylammonium chloride tetrahydrate [31] and anhydrous tetraethylammonium chloride [32]. The lengths of the N-C bonds are in the range between 1.512 (3) (N-Cl) and 1.516 (3) Å (N-C3). The lengths of the other two N-C bonds are equal to 1.522 (3) Å. The C-N-C angles are in between 106.5(2) to 111.1(2)°. The C-C bonds lengths are in the region between 1.509(4) and 1.517(4). Thus, they are very similar. The final coordinates and U_{eq} or U_{iso} of TEP are given in **Table 4**.

3.2. Vibrational Investigations

The FT-IR and FT-Raman spectra of the title crystal were measured for the powder sample at room temperature. The bands observed in the measured region arise from the vibrations of hydrogen bonds, vibrations of the tetrapropylammonium cation, phosphate groups, and lattice vibrations. Vibrational spectra are shown in **Fig-**

ures 3 and 4.

3.2.1. The Hydrogen Bond Vibrations

The valence vibrations of O-H groups interconnected by a system of hydrogen bonds in the crystal appear in IR spectrum as broad bands in the 3500 - 1800 cm^{-1} region [15]. As can be seen from **Table 3**, these consist of hydrogen bonds of O-H \cdots O type with length ranging from 2.521(2) to 2.617 (2) Å. X-ray data show that H atoms of OH groups generate hydrogen bonds with the oxygen atoms of the PO_4 group.

The stretching type of vibrations of hydrogen bonds νOH displays a well defined and medium intense band in IR with the AB structure in the region between 3500 and 2000 cm^{-1} . In IR spectrum the frequency of A band is 2750 cm^{-1} and B is 2460 cm^{-1} . For Raman experiment the broad maxima are found at 2822 and 2550 cm^{-1} . The intense IR bands correspond to a strong hydrogen bond with the O \cdots O distance in the region 2.6 Å - 2.7 Å [33]. The in-plane OH bending mode δOH gives rise to a medium band in infrared spectrum without counterparts in Raman spectrum at 1252 cm^{-1} . The out-of-plane bending

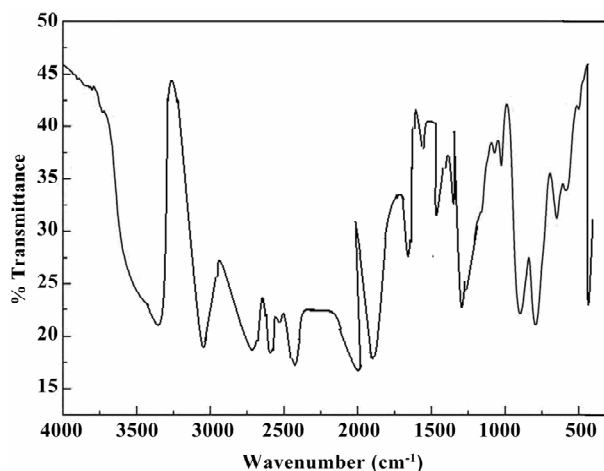


Figure 3. IR spectrum of $[\text{CH}_3\text{CH}_2]_4\text{N}(\text{H}_2\text{PO}_4)(\text{H}_3\text{PO}_4)_2$.

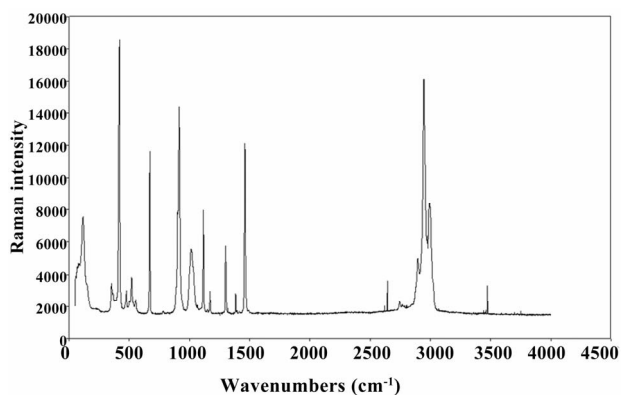


Figure 4. Raman spectrum of $[\text{CH}_3\text{CH}_2]_4\text{N}(\text{H}_2\text{PO}_4)(\text{H}_3\text{PO}_4)_2$.

Table 4. Principal intratomic distances (Å) and bond angles (°) in $[\text{CH}_3\text{CH}_2]_4\text{N}^+(\text{H}_2\text{PO}_4^-)(\text{H}_3\text{PO}_4)_2$ $U_{\text{eq}} = \frac{1}{3} \sum_i \sum_j U_{ij} a_i^* a_j^* a_i a_j$.

Atoms	x/a	y/b	z/c	Ueq or Uiso*
P1	0.15869 (7)	0.49303 (4)	0.13317 (4)	0.0127 (2)
P2	0.70980 (7)	0.49978 (4)	0.2963 (4)	0.0113 (2)
P3	0.20672 (7)	0.42355 (4)	0.4170 (4)	0.0114 (2)
O (1)	0.2430 (2)	0.4957 (1)	0.0464 (1)	0.0196 (4)
O (2)	-0.0332 (2)	0.5117 (1)	0.1105 (1)	0.0198 (4)
O (3)	0.1999 (2)	0.4066 (1)	0.1727 (1)	0.0181 (4)
O (4)	0.2539 (2)	0.5555 (1)	0.2025 (1)	0.0174 (4)
O (5)	0.8479 (2)	0.5531 (1)	0.3526 (1)	0.0139 (4)
O (6)	0.5279 (2)	0.5109 (1)	0.3156 (1)	0.0149 (4)
O (7)	0.6960 (2)	0.5166 (1)	0.1917 (1)	0.0238 (5)
O (8)	0.7616 (2)	0.4086 (1)	0.3146 (1)	0.0194 (4)
O (9)	0.1654 (2)	0.3748 (1)	0.4992 (1)	0.0150 (4)
O (10)	0.4068 (2)	0.4171 (1)	0.4239 (1)	0.0185 (4)
O (11)	0.1023 (2)	0.38909 (1)	0.3296 (1)	0.0153 (4)
O (12)	0.1651(2)	0.51456 (1)	0.4281 (1)	0.0165 (4)
H1	0.171(6)	0.492 (3)	0.002 (3)	0.065 (15)*
H3	0.165(6)	0.404 (3)	0.218 (3)	0.073 (14)*
H4	0.350(5)	0.541 (2)	0.235 (3)	0.051 (11)*
H6	0.4600(2)	0.4802 (3)	0.2829 (2)	0.022 (11)*
H7	0.793(5)	0.514 (2)	0.178 (3)	0.048 (11)*
H9	0.180(5)	0.401 (3)	0.550 (3)	0.064 (13)*
H10	0.446(5)	0.446 (2)	0.392 (2)	0.045 (11)*
H12	0.063(5)	0.527 (2)	0.403 (3)	0.042 (10)*
n	0.6747(2)	0.2404 (1)	0.5702 (1)	0.0159 (4)
C (1)	0.8236 (3)	0.2084 (2)	0.6421 (2)	0.0200 (5)
C (2)	0.5598 (3)	0.1684 (2)	0.5342 (2)	0.0217 (5)
C (3)	0.7439 (3)	0.2823 (2)	0.4926 (2)	0.0180 (5)
C (4)	0.5705 (3)	0.3036 (2)	0.6116 (2)	0.0172 (5)
C (5)	0.8522 (4)	0.2285 (2)	0.4423 (2)	0.0251 (6)
C (6)	0.9576 (3)	0.2711 (2)	0.6843 (2)	0.0259 (6)
C (7)	0.4887 (4)	0.2736 (2)	0.6904 (2)	0.0250 (6)
C (8)	0.4006 (4)	0.1887 (2)	0.4623 (2)	0.0314 (7)
H (1A)	0.879 (4)	0.169 (2)	0.6136 (19)	0.024 (7)*
H (1B)	0.768 (3)	0.182 (2)	0.6914 (18)	0.022 (7)*
H (2A)	0.627 (4)	0.127 (2)	0.5076 (19)	0.023 (7)*
H (2B)	0.527 (3)	0.143 (2)	0.5870 (18)	0.018 (7)*
H (3A)	0.811 (4)	0.324 (2)	0.517 (2)	0.028 (8)*
H (3B)	0.641 (3)	0.301 (2)	0.4522 (18)	0.015 (6)*
H (4A)	0.653 (3)	0.348 (2)	0.632 (2)	0.017 (7)*
H (4B)	0.483 (3)	0.321 (2)	0.564 (2)	0.012 (6)*
H (5A)	0.948 (4)	0.207 (2)	0.482 (2)	0.023 (7)*
H (5B)	0.787 (4)	0.185 (2)	0.411 (2)	0.029 (8)*
H (5c)	0.897 (4)	0.263 (2)	0.396 (2)	0.025 (7)*
H (6A)	1.020 (4)	0.292 (2)	0.641 (2)	0.029 (8)*
H (6B)	0.903 (4)	0.312 (2)	0.715 (2)	0.041 (9)*
H (6C)	1.040 (4)	0.244 (2)	0.729 (2)	0.035 (8)*

Continued

H (7A)	0.576 (4)	0.258 (2)	0.737 (2)	0.031 (8)*
H (7B)	0.406 (4)	0.233 (2)	0.671 (2)	0.027 (8)*
H (7C)	0.420 (4)	0.318 (2)	0.708 (2)	0.030 (8)*
H (8A)	0.429 (4)	0.212 (2)	0.409 (2)	0.036 (9)*
H (8B)	0.348 (5)	0.137 (3)	0.448 (3)	0.062 (1)*
H (8C)	0.311 (5)	0.225 (3)	0.483 (3)	0.064 (1)*

* is relatif to Uiso of hydrogen.

γ OH mode appears in the region 900 and 700 cm^{-1} , but is not observed in spectra measured at ambient temperature.

3.2.2. The Tetraethylammonium Cation Vibrations

The frequencies observed in the infrared spectra at 2977 and 2957 cm^{-1} are assigned to the δ symmetric CH_2 and δ asymmetric CH_3 absorptions; the different modes of asymmetric (δ_{as}) and symmetric (δ_{s}) deformation of the methyl groups are found at 1495 and 1397 cm^{-1} , respectively. A weak band which appeared at 1323 cm^{-1} is related to the N-C vibration [34,35]. Besides, sharp bands at 1196, 1172 and 1102, 1116 cm^{-1} are associated to CH_3 and CH_2 rocking vibration modes in IR and spectively. The two bands observed at 952 cm^{-1} in IR and 915 cm^{-1} in Raman were assigned to $\nu_1(\text{NC}_4)$ stretch Raman, reing modes [36-38]. The deformation mode $\nu_2(\text{NC}_4)$ appears at 744 and 672 cm^{-1} in IR and Raman spectrum, respectively. The splitting ν (C-C-C-N) bending mode at 772 cm^{-1} may correspond to different conformers of the organic chains. The band observed at 463 cm^{-1} in infrared and 478 cm^{-1} in Raman spectrum arises from the deformation vibration $\nu_4(\text{NC}_4)$ of the TEP entity.

3.2.3. Internal Vibrations of the Phosphate Groups

The unperturbed PO_4^{3-} ion is a tetrahedron with a point group symmetry T_d . The ν_1 (A) and ν_3 (F₂) symmetric and asymmetric stretching modes are observed in 1000 - 700 cm^{-1} region, whereas the ν_2 (E) and ν_4 (F₂) symmetric and asymmetric bending modes are distinguished in the 500 - 400 cm^{-1} domain [39,40].

The interpreting of the IR and Raman spectrum is made in terms of internal modes of two atomic groups, PO_2 and $\text{P}(\text{OH})_2$, included in H_2PO_4^- anion. The two stretching vibrations, asymmetric and symmetric of PO_2 group, are observed in the region 1065 - 895 cm^{-1} ; while those related to $\text{P}(\text{OH})_2$ group occur as two intense bands in the domain 1000 - 861 cm^{-1} . The splitting of F₂ stretching mode of PO_4 , into three intense components at 1059, 1032, 889 cm^{-1} is a strong evidence of the symmetry lowering of H_2PO_4^- in the solid state. On the other hand, bending modes of H_2PO_4^- group are observed at lower frequencies. The bands located in the region 487 - 400 cm^{-1} , are respectively attributed to the torsion $\rho(\text{PO}_2)$, to the wagging $\omega(\text{PO}_2)$, and to the bending $\delta[\text{P}(\text{OH})_2]$ vibrations.

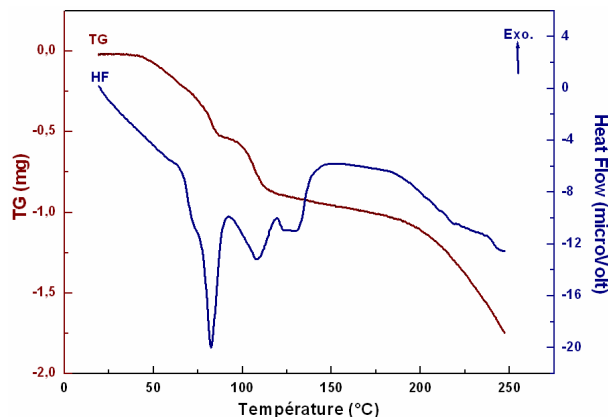


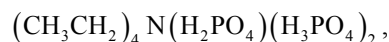
Figure 5. The TG-DSC curve of $[\text{CH}_3\text{CH}_2]_4\text{N}(\text{H}_2\text{PO}_4)(\text{H}_3\text{PO}_4)_2$.

3.3. Thermal Analysis (DSC and ATG)

DSC-ATG of TEP was done in air at the rate of 5°C/min. One more characteristic feature of the room temperature TEP is its high hygroscopicity (Figure 5), which illustrates the calorimetric (DSC) and thermogravimetric (TGA) results. This compound is stable until 320 K, above this temperature, or loss of weight appears at 355 K and 381 K. It is due to the departure of adsorbed water. The endothermic peak observed at $T = 401$ K is attributed to the melting of TEP.

4. Conclusions

Crystals of a hybrid material,



have been prepared by slow evaporation of aqueous solution $(\text{CH}_3\text{CH}_2)_4\text{NOH}$ and H_3PO_4 at room temperature.

The structure consists of strong two dimensional character based on sheets of H_2PO_4^- and H_3PO_4 tetrahedra fused together by strong intralayer O-H...O hydrogen bonds, giving to trimmers. The planes of inorganic groups alternate with planes of organic cations. In addition, the two layers spreading in this network are themselves interconnected by strong O-H...O and C-H...O hydrogen bonding.

Vibrational study recorded is of great interest as it

verifies the dependence of groups constituting our material. The hydrogen bonds confirmed by IR and X-Ray diffraction explain the stability of our compound.

REFERENCES

- [1] L. Baouab and A. Jouini, "Crystal Structures and Thermal Behavior of Two New Organic Monophosphates," *Journal of Solid State Chemistry*, Vol. 141, No. 2, 1998, pp. 343-351. [doi:10.1006/jssc.1998.7933](https://doi.org/10.1006/jssc.1998.7933)
- [2] M. T. Averbuch-Pouchot and A. Durif, "Structures of Ethylenediammonium Monohydrogentetraoxophosphate(V) and Ethylenediammonium Monohydrogentetraoxoarsenate(V)," *Acta Crystallographica*, Vol. C43, 1987, pp. 1894-1896. [doi:10.1107/S0108270187089716](https://doi.org/10.1107/S0108270187089716)
- [3] M. T. Averbuch-Pouchot, A. Durif and J. C. Guitel, "Structures of -Alanine, DL-Alanine and Sarcosine Monophosphates," *Acta Crystallographica*, Vol. C44, 1988, pp. 1968-1972. [doi:10.1107/S0108270188000502](https://doi.org/10.1107/S0108270188000502)
- [4] M. T. Averbuch-Pouchot, A. Durif and J. C. Guitel, "Structures of Glycine Monophosphate and Glycine Cyclo-Triphosphate," *Acta Crystallographica*, Vol. C44, 1988, pp. 99-102. [doi:10.1107/S0108270187008539](https://doi.org/10.1107/S0108270187008539)
- [5] M. Bagieu-Beucher, "Structure of Cytosinium Dihydrogenmonophosphate," *Acta Crystallographica*, Vol. C46, 1990, p. 238.
- [6] R. H. Blessing, "Hydrogen Bonding and Thermal Vibrations in Crystalline Phosphate Salts of Histidine and Imidazole," *Acta Crystallographica*, Vol. B42, 1986, pp. 613-621. [doi:10.1107/S0108768186097641](https://doi.org/10.1107/S0108768186097641)
- [7] M. T. Averbuch-Pouchot, A. Durif and J. C. Guitel, "Structure of Ethylenediammonium Dihydrogentetraoxophosphate(V) Pentahydrogenbis[Tetraoxophosphate(V)]," *Acta Crystallographica*, Vol. C45, 1989, pp. 421-423. [doi:10.1107/S0108270188011977](https://doi.org/10.1107/S0108270188011977)
- [8] S. Kamoun, M. Kamoun, A. Jouini and A. Daoud, "Structure of Ethylenediammonium Bis(Dihydrogenmonophosphate)," *Acta Crystallographica*, Vol. C45, 1989, pp. 481-482. [doi:10.1107/S0108270188012405](https://doi.org/10.1107/S0108270188012405)
- [9] M. Bagieu-Beucher, A. Durif and J. C. Guitel, "Structure of Ethylenediammonium Dihydrogentetraoxophosphate(V) Pentahydrogenbis[tetraoxophosphate(V)]," *Acta Crystallographica*, Vol. C43, 1989, pp. 421-423. [doi:10.1107/S0108270188011977](https://doi.org/10.1107/S0108270188011977)
- [10] S. Kamoun, A. Jouini and A. Daoud, "Structure du Propanediammonium-1,3 Monohydrogénomonophosphate Monohydrate," *Acta Crystallographica*, Vol. C47, 1991, pp. 117-119. [doi:10.1107/S0108270190003122](https://doi.org/10.1107/S0108270190003122)
- [11] S. Kamoun, A. Jouini, A. Daoud, A. Durif and J. C. Guitel, "Structure du Diammonium-1,3 Propane Bis(Dihydrogénomonophosphate)," *Acta Crystallographica*, Vol. C48, 1992, pp. 133-135. [doi:10.1107/S0108270191008077](https://doi.org/10.1107/S0108270191008077)
- [12] S. Kamoun and A. Jouini, "Etude Calorimétrique et Structure Cristalline du Putrescine Monohydrogénomonophosphate Dihydrate $\text{NH}_3(\text{CH}_2)_4\text{NH}_3\text{HPO}_4 \cdot 2\text{H}_2\text{O}$," *Journal of Solid State Chemistry*, Vol. 89, No. 1, 1990, pp. 67-74. [doi:10.1016/0022-4596\(90\)90294-8](https://doi.org/10.1016/0022-4596(90)90294-8)
- [13] F. Takusagaxa and T. F. Koetzle, "A Study of the Charge Density in Putrescine Diphosphate at 85 K," *Acta Crystallographica*, Vol. B35, 1979, pp. 867-877. [doi:10.1107/S0567740879005082](https://doi.org/10.1107/S0567740879005082)
- [14] Z. Elaoud, S. Kamoun, T. Mhiri and J. J. Jaud, "Crystal Structure of Triethyltetraammonium Bis Monohydrogenmonophosphate Dihydrate, $[\text{NH}_3(\text{CH}_2)_2\text{NH}_2(\text{CH}_2)_2\text{NH}_2(\text{CH}_2)_2\text{NH}_3](\text{HPO}_4)_2 \cdot 2\text{H}_2\text{O}$," *Journal of Chemical Crystallography*, Vol. 29, 1999, pp. 541-545.
- [15] Z. Elaoud, S. Kamoun, T. Mhiri, F. Romain and H. J. Burzlaff, "Crystal Structure and Phase Transitions in N-benzyl Piperidinium Dihydrogenmonophosphate, $\text{C}_6\text{H}_5\text{CH}_2\text{CHCH}_2\text{CH}_2\text{NH}_2\text{CH}_2\text{CH}_2 \cdot \text{H}_2\text{PO}_4$," *Journal of Solid State Chemistry*, Vol. 155, 2000, pp. 298-304.
- [16] Z. Elaoud, S. Kamoun, J. J. Jaud and T. Mhiri, "Crystal Structure of N-benzylmethylammonium Dihydrogen-Monophosphate Monohydrate, $[\text{C}_6\text{H}_5\text{CH}_2\text{NH}_2\text{CH}_3]\text{H}_2\text{PO}_4 \cdot \text{H}_2\text{O}$," *Journal of Chemical Crystallography*, Vol. 28, 1998, pp. 313-315. [doi:10.1023/A:1021861621824](https://doi.org/10.1023/A:1021861621824)
- [17] S. Kamoun, A. Jouini and A. Daoud, "Structure du Aza-3 Pentanediyole-1,5 Diammonium Monohydrogénomonophosphate Dihydrate," *Acta Crystallographica*, Vol. C46, 1990, pp. 1481-1483. [doi:10.1107/S0108270189012552](https://doi.org/10.1107/S0108270189012552)
- [18] S. Kamoun, A. Daoud, A. Elfakir, M. Quarton and I. Ledoux, "Linear and Nonlinear—Optical Properties on N-Diethylendiammonium Monohydrogenophosphate Dihydrate," *Journal of Solid State Chemistry*, Vol. 94, 1995, pp. 893-896.
- [19] C. Lee and W. T. A. Harrison, "Tetraethylammonium Dihydrogenarsenate Bis(Arsenic Acid) and 1,4-Diazoniabicyclo[2.2.2]octane Bis(Dihydrogenarsenate) Arsenic Acid: Hydrogen-Bonded Networks Containing Dihydrogenarsenate Anions and Neutral Arsenic Acid Molecules," *Acta Crystallographica*, Vol. C63, 2007, pp. m308-m311. [doi:10.1107/S0108270107023967](https://doi.org/10.1107/S0108270107023967)
- [20] G. Charlot, "Chimie Analytique Quantitative," Vol. 2, Masson and Cie, Paris, 1974.
- [21] E. A. Muller, R. J. Cannon, A. N. Sarjeant, K. M. Ok, P. S. Halasyamani and A. J. Norquist, "Directed Synthesis of Noncentrosymmetric Molybdates," *Crystal Growth & Design*, Vol. 5, No. 5, 2005, pp. 1913-1917. [doi:10.1021/cg050184z](https://doi.org/10.1021/cg050184z)
- [22] Nonius, "Kappa CCD Program Software," Nonius BV, Delft, 1998.
- [23] L. J. Farrugia, "WinGX Suite for Small-Molecule Single-Crystal Crystallography," *Journal of Applied Crystallography*, Vol. 32, 1999, p. 837. [doi:10.1107/S0021889899006020](https://doi.org/10.1107/S0021889899006020)
- [24] G. M. Sheldrick, "SHELXS-97 Programs for Crystal Solution," University of Göttingen, Göttingen, 1997.
- [25] G. M. Sheldrick, "SHELXL-97 Programs for Crystal Structure Refinement," University of Göttingen, Göttingen, 1997.
- [26] I. D. Brown, "On the Geometry of O-H...O Hydrogen Bonds," *Acta Crystallographica*, Vol. A32, 1976, pp. 24-31. [doi:10.1107/S0567739476000041](https://doi.org/10.1107/S0567739476000041)

- [27] R. H. Blessing, "Hydrogen Bonding and Thermal Vibrations in Crystalline Phosphate Salts of Histidine and Imidazole," *Acta Crystallographica*, Vol. B42, 1986, pp. 613-621. [doi:10.1107/S0108768186097641](https://doi.org/10.1107/S0108768186097641)
- [28] J. Baran, M. Śledź, M. Drozd, A. Pietraszko, A. Haznar and H. Ratajczak, "Structural, Vibrational and DSC Investigations of the Tetraethylammonium Hydrogensele-nate Crystal," *Journal of Molecular Structure*, Vol. 526, 2000, pp. 361-371. [doi:10.1016/S0022-2860\(00\)00530-5](https://doi.org/10.1016/S0022-2860(00)00530-5)
- [29] E. Steinwender, E. T. G. Lutz, J. H. van der Maas and J. A. Kanters, "2-Ethynyladamantan-2-ol: A Model Compound with Distinct $\text{OH}\cdots\pi$ and $\text{CH}\cdots\text{O}$ Hydrogen Bonds," *Vibrational Spectroscopy*, Vol. 4, No. 2, 1993, pp. 217-229. [doi:10.1016/0924-2031\(93\)87041-Q](https://doi.org/10.1016/0924-2031(93)87041-Q)
- [30] J. H. Loehlin and A. Kvik, "Tetraethylammonium Chloride Monohydrate," *Acta Crystallographica*, Vol. B34, 1978, pp. 3488-3490. [doi:10.1107/S0567740878011425](https://doi.org/10.1107/S0567740878011425)
- [31] T. C. W. Mak, H. J. B. Slot and P. T. Beurskens, "Tetra-ethylammonium Chloride Tetrahydrate, a 'Double Chan-nel' Host Lattice Constructed from $(\text{H}_2\text{O})_4\text{Cl}^-$ Tetrahedra Linked between Vertices," *Journal of Inclusion Phenom-ena*, Vol. 4, No. 3, 1986, p. 295. [doi:10.1007/BF00658004](https://doi.org/10.1007/BF00658004)
- [32] R. J. Staples and Z. Kristallogr, "Crystal Structure of 4,4-Dimethyloxazolidine-2-Thione, $\text{C}_5\text{H}_9\text{NOS}$," *NCS*, 1999, pp. 214-231.
- [33] A. Novak, "Hydrogen Bonding in Solids Correlation of Spectroscopic and Crystallographic Data," *Structure and Bonding*, Vol. 18, 1974, pp. 177-178. [doi:10.1007/BFb0116438](https://doi.org/10.1007/BFb0116438)
- [34] M. Gosniowska, Z. Ciunik, G. Bator, R. Jakubas and J. Baran, "Structure and Phase Transitions in Tetramethy-lammonium Tetrabromoindate(III) and Tetraethylammon-ium Tetrabromoindate(III) Crystals," *Journal of Mole-cular Structure*, Vol. 555, 2000, p. 243. [doi:10.1016/S0022-2860\(00\)00607-4](https://doi.org/10.1016/S0022-2860(00)00607-4)
- [35] M. Karbowski, J. Hanuza, J. Janczak and J. Drozdzyński, "Synthesis, Structural and Spectroscopic Properties of Tetra(Tetraethylammonium) Heptaisothiocyanato Uranate (III) and Neodymate(III)," *Journal of Alloys and Com-pounds*, Vol. 225, 1995, p. 338. [doi:10.1016/0925-8388\(94\)07117-9](https://doi.org/10.1016/0925-8388(94)07117-9)
- [36] H. G. Heddrich and C. E. Blom, "Flame Diagnostics and Molecular Constants of CaO by Tunable Diode Laser Spectroscopy," *The Journal of Chemical Physics*, Vol. 90, 1989, p. 4660. [doi:10.1063/1.456610](https://doi.org/10.1063/1.456610)
- [37] H. G. Heddrich and C. E. Blom, "The Infrared Spectrum of Barium Oxide in the Gas Phase," *Journal of Molecular Spectroscopy*, Vol. 140, 1990, p. 103. [doi:10.1016/0022-2852\(90\)90009-F](https://doi.org/10.1016/0022-2852(90)90009-F)
- [38] A. D. Kirkwood, K. D. Bier, J. K. Thompson, T. L. Has-lett, A. S. Hubber and M. Moskovits, "Ultraviolet-Visible and Raman Spectroscopy of Diatomic Manganese Iso-lated in Rare-Gas Matrixes," *The Journal of Chemical Physics*, Vol. 95, 1991, p. 2644. [doi:10.1021/j100160a006](https://doi.org/10.1021/j100160a006)
- [39] G. Ma, T. Zhang, K. Yu and J. Braz, "Synthesis, X-Ray Crystal Structure and Thermal Decomposition Mecha-nism of $[\text{Zn}(\text{MCZ})_3](\text{NO}_3)_2\cdot\text{H}_2\text{O}$ (MCZ=Methyl Carba-zate)," *Journal of the Brazilian Chemical Society*, Vol. 16, 2005, p. 796. [doi:10.1590/S0103-50532005000500018](https://doi.org/10.1590/S0103-50532005000500018)
- [40] M. Drozd, "The Equilibrium Structures, Vibrational Spec-tra, NLO and Directional Properties of Transition Dipole Moments of Diguandinium Arsenate Monohydrate and Diguandinium Phosphate Monohydrate: The Theoretical DFT Calculations," *Spectrochimica Acta Part A*, Vol. 65, No. 5, 2006, pp. 1069-1086. [doi:10.1016/j.saa.2006.02.007](https://doi.org/10.1016/j.saa.2006.02.007)

Supplementary Material

CCDC831725 contains the supplementary crystallogra-
phic data for 1. These data can be obtained free of charge
via www.ccdc.cam.ac.uk/data_request/cif or by emailing

data_request@ccdc.cam.ac.uk, or by contacting the Cam-
bridge Crystallography Data Centre 12, Union Road,
Cambridge CB2 1EZ, UK [Fax: +441223336030].